



## City Research Online

### City, University of London Institutional Repository

---

**Citation:** Giaralis, A. & Spanos, P. D. (2012). Derivation of response spectrum compatible non-stationary stochastic processes relying on Monte Carlo-based peak factor estimation. *Earthquakes and Structures*, 3(3\_4), pp. 581-609. doi: 10.12989/eas.2012.3.3\_4.581

This is the accepted version of the paper.

This version of the publication may differ from the final published version.

---

**Permanent repository link:** <https://openaccess.city.ac.uk/id/eprint/925/>

**Link to published version:** [https://doi.org/10.12989/eas.2012.3.3\\_4.581](https://doi.org/10.12989/eas.2012.3.3_4.581)

**Copyright:** City Research Online aims to make research outputs of City, University of London available to a wider audience. Copyright and Moral Rights remain with the author(s) and/or copyright holders. URLs from City Research Online may be freely distributed and linked to.

**Reuse:** Copies of full items can be used for personal research or study, educational, or not-for-profit purposes without prior permission or charge. Provided that the authors, title and full bibliographic details are credited, a hyperlink and/or URL is given for the original metadata page and the content is not changed in any way.

---

---

---

City Research Online:

<http://openaccess.city.ac.uk/>

[publications@city.ac.uk](mailto:publications@city.ac.uk)

---

# Derivation of response spectrum compatible non-stationary stochastic processes relying on Monte Carlo-based peak factor estimation

AGATHOKLIS GIARALIS<sup>1</sup> and POL D. SPANOS<sup>2</sup>

<sup>1</sup>*School of Engineering and Mathematical Sciences, City University London, Northampton Square, EC1V0HB, London, UK*

*E-mail: agathoklis@city.ac.uk*

<sup>2</sup>*Department of Mechanical Engineering and Material Sciences, Rice University, 6100 Main St, Houston, TX 77251, USA*

*E-mail: spanos@rice.edu*

**Abstract:** In this paper a novel approach is proposed to address the problem of deriving non-stationary stochastic processes which are compatible in the mean sense with a given (target) response (uniform hazard) spectrum (UHS) as commonly desired in the aseismic structural design regulated by contemporary codes of practice. The appealing feature of the approach is that it is non-iterative and “one-step”. This is accomplished by solving a standard over-determined minimization problem in conjunction with appropriate median peak factors. These factors are determined by a plethora of reported new Monte Carlo studies which on their own possess considerable stochastic dynamics merit. In the proposed approach, generation and treatment of samples of the processes individually on a deterministic basis is not required as is the case with the various “two-step” approaches found in the literature addressing the herein considered task. The applicability and usefulness of the approach is demonstrated by furnishing extensive numerical data associated with the elastic design UHS of the current European (EC8) and the Chinese (GB 50011) aseismic code provisions. Purposely, simple and thus attractive from a practical viewpoint, uniformly modulated processes assuming either the Kanai-Tajimi (K-T) or the Clough-Penzien (C-P) spectral form are employed. The Monte Carlo studies yield damping and duration dependent median peak factor spectra, given in a polynomial form, associated with the first passage problem for UHS compatible K-T and C-P uniformly modulated stochastic processes. Hopefully, the herein derived stochastic processes and median peak factor spectra can be used to facilitate the

aseismic design of structures regulated by contemporary code provisions in a Monte Carlo simulation-based or stochastic dynamics-based context of analysis.

**Keywords:** non-stationary process, design spectrum compatible, inverse problem, Monte Carlo simulation, peak factors, artificial accelerograms.

## 1. Introduction

In the practice of aseismic design of structures, the concept of the elastic response spectrum has been traditionally used to describe the hazard posed by seismic events on structures (e.g. Chopra 2007). Furthermore, inelastic response spectra of reduced spectral ordinates are utilized to account for the expected hysteretic behavior of structures exposed to extreme seismic loads (e.g. Newmark and Hall 1982). In fact, aseismic code provisions represent the input seismic loads by means of analytically defined (uniform hazard) response/design spectra (UHS) (e.g. CEN 2004, ASCE 2006). The practice of using response/design elastic/inelastic spectra allows for considering linear dynamic response-spectrum based types of analyses which significantly facilitates the design of “ordinary/regular” structures.

Nevertheless, additional dynamic linear and non-linear time-history analyses are further mandated by regulatory agencies to be performed in the design of “special” and/or “non-regular” structured facilities (e.g. CEN 2004, ASCE 2000, ASCE 2006, GB 50011 2001). These analyses require the consideration of small suites of accelerograms (commonly three to seven pairs of accelerograms) whose average response spectrum lies close to (i.e. is compatible with) the elastic response/design UHS. Two common approaches to obtain such accelerograms is either by careful selection and, if needed, scaling of field recorded signals (see e.g. Katsanos et al 2010, Jayaram et al 2011, and references therein), or by generation of

simulated time-histories compatible with power spectra which are consistent with the design spectrum (see e.g. Preumont 1985a, Giaralis and Spanos 2009, Cacciola 2010, Martinelli et al. 2011, and references therein). The consensus in the earthquake engineering community is to use field recorded accelerograms over simulated ones to account for the uncertainty of the non-stationary attributes (i.e. the time-dependent amplitude and frequency content) observed in strong ground motions. However in some cases the availability of seismic records satisfying certain seismological and site soil conditions criteria may be limited (e.g. Iervolino et al. 2008). This may be a rather important issue especially in cases where a large number of records is required to be used within a Monte Carlo simulation-based analysis (e.g. Taflanidis and Jia 2011). Moreover, in certain other cases, random vibration analyses may be deemed essential to be included in the aseismic design process (e.g. Wen and Eliopoulos 1994). The aforementioned cases call for a representation of the input seismic excitation by an appropriately defined response/design UHS compatible stochastic process.

In this context, various researchers have proposed methods to relate a response/design spectrum to a power spectrum characterizing a stationary random process (see e.g. Kaul 1978, Gupta and Trifunac 1998, Falsone and Neri 2000, Giaralis and Spanos 2010 and references therein). Such a relation involves the consideration of the so-called peak factor which is closely associated with the first passage problem of the response of stochastically excited linear single-degree-of-freedom (SDOF) systems (e.g. Vanmarcke 1976). This problem is not amenable to a general closed form solution, but for the stationary case there are reliable semi-empirical expressions for the peak factor (e.g. Vanmarcke 1976, Preumont 1985b).

Arguably, assigning a stationary process to a response/design spectrum involves a rather restrictive limitation in dealing with an inherently non-stationary phenomenon (i.e. the strong ground motion during a seismic event). Nevertheless, limited research work has been

devoted to relating an evolutionary power spectrum (EPS) characterizing a non-stationary random process as defined by Priestley (1965) directly to a given response/design spectrum (e.g. Preumont 1985a, Spanos and Vargas Loli 1985 ). The main difficulty in this case, is that there are not reliable approximate expressions for the peak factor. Some previous studies (e.g. Corotis et al. 1972, Mason and Iwan 1983, Zembaty 1988, Senthilnathan and Lutes 1991, Michaelov et al. 2001, Morikawa and Zerva 2008) have provided numerical results associated with the peak response and the first passage problem of linear SDOF systems excited by non-stationary input. However, the considered input EPSs have been arbitrarily selected as either modulated white noise, or colored noise having a boxcar envelop function (essentially dealing with the transient and not the non-stationary response). Obviously, these forms of EPSs do not correspond to non-stationary processes consistent with a particular seismic response spectrum.

To circumvent the need to consider peak factors for non-stationary input processes, most research studies use an indirect two-step approach to address the issue of deriving simulated accelerograms compatible with a UHS (e.g. Gupta and Joshi 1993, Shrikhade and Gupta 1996, Crespi et al. 2002, Martinelli et al. 2011). First, a stationary power spectrum is “fit” to the target response spectrum, usually through an iterative procedure. Then, stationary time-histories compatible with the initially obtained power spectrum are generated and treated deterministically on an individual basis to assign certain non-stationary attributes similar to those observed in field recorded accelerograms. Alternatively, Cacciola (2010) has considered fitting the sum of two contributing processes to the UHS, namely a stationary power spectrum and a scaled time-frequency energy distribution of a single recorded seismic accelerogram using the spectral estimation method of Conte and Peng (1997). The aforementioned studies are useful in deriving small suites of design spectrum compatible accelerograms. However, they do not address the issue of obtaining a UHS compatible

nonstationary stochastic process represented by an analytically defined EPS in a direct fashion. Note that such processes can be used in a straightforward manner for random vibration-based or for Monte Carlo simulation-based kinds of analysis for the design of structures regulated by specific codes of practice.

In this regard, this study first adopts an inverse stochastic dynamics formulation originally proposed by Spanos and Vargas Loli (1985) to fit an analytically defined EPS directly to a given response spectrum. This is accomplished in a non-iterative one-step manner by relying on the solution of a standard over-determined optimization problem. The latter involves the consideration of a peak factor to establish statistically the nature of compatibility between the EPS and the target spectrum. Non-constant median frequency-dependent peak factors (median peak factor spectra) consistent with the given target spectrum are employed in the solution of the aforementioned problem. These peak factor spectra are derived numerically by a plethora of pertinent Monte Carlo analyses to circumvent the lack of a dependable semi-empirical expression as previously mentioned. Base-line corrected EPS compatible accelerograms are obtained by an efficient random field simulation technique to ensure that an acceptable level of compatibility of the derived processes with the target response spectrum in the mean sense is achieved. This is an issue of practical importance as common codes of practice mandate such a kind of compatibility with the UHS in representing the seismic action for analyses different than the response-spectrum based ones, as has been already discussed. Furthermore, the adopted parametric form of the EPS is, purposely, kept as simple as possible to be attractive for practical design purposes within a random vibration based or a Monte Carlo based kind of analysis. It contains enough “degrees-of-freedom” to accommodate a physically meaningful solution of the considered inverse stochastic dynamics problem. In particular, it involves a relatively simple deterministic time-varying envelop

function modulating a stationary power spectrum expressed either by the Kanai-Tajimi (K-T) (Kanai 1957) or by the Clough-Penzien (C-P) (Clough and Penzien 1993) spectral form.

It is emphasized that this work does not intend to address the issue of deriving small suites of design spectrum compatible accelerograms to be used for inelastic time-history analysis as mandated by aseismic code provisions for the case of certain kinds of structures. This topic has been extensively addressed in the published literature by the authors (Giaralis and Spanos 2009, Spanos et al. 2009) and by many other researchers already cited. Rather, its main objective is to demonstrate, by furnishing extensive numerical data, the potential of the adopted formulation combined with appropriately derived median peak factor spectra to obtain UHS compatible nonstationary stochastic processes in a direct manner without the need to further generate and treat samples of the underlying stochastic process individually on a deterministic basis.

In what follows, a brief review of the mathematical background on the adopted formulation is included in section 2. Section 3 focuses on the Monte Carlo-based estimation of median peak factor spectra. These are used in conjunction with the adopted formulation to obtain non-stationary processes achieving enhanced compatibility with the target spectrum. The elastic UHS prescribed by the European EC8 (CEN 2004) code provisions is used as a paradigm of a target spectrum. Section 4 provides numerical evidence on the applicability of the adopted formulation to derive non-stationary processes with pre-specified “effective duration” as defined by Trifunac and Brady (1975). In this case the UHS prescribed by the Chinese GB 50011 (GB 50011 2001) code provisions is set to be the target spectrum. Section 5 discusses in light of numerical data pertaining to both the EC8 spectrum and the GB 50011 spectrum that the selection of an appropriate spectral depends on the definition of the “target” UHS in the region of relatively long periods. Finally, section 6 includes a summary of

conclusions and remarks highlighting the practical merit of the proposed approach and of the herein reported numerical results.

## 2. Mathematical Background

To ensure the completeness of this paper, this section briefly reviews the adopted theoretical concepts and mathematical formulations used in deriving the numerical data presented in ensuing sections. More details on the herein considered formulation can be found in Spanos and Vargas Loli (1985) and in Giaralis and Spanos (2009).

### 2.1. Assumed time and frequency domain attributes of the sought stochastic processes

Let the acceleration trace of the strong ground motion due to an earthquake be modeled as a realization of a modulated non-stationary stochastic process  $u_g(t)$ . That is,

$$u_g(t) = A(t)y(t), \quad (1)$$

where  $A(t)$  is a deterministic envelop function dependent on time  $t$  and  $y(t)$  is a zero-mean stationary stochastic process. For sufficiently “slowly-varying” envelop functions, the process  $u_g(t)$  can be reliably represented in the domain of frequencies  $\omega$  by a two-sided evolutionary power spectrum (EPS)  $G(t,\omega)$  given by the expression (Priestley 1965)

$$G(t,\omega) = |A(t)|^2 Y(\omega), |\omega| \leq \omega_b, \quad (2)$$

where  $\omega_b$  is the highest frequency contained in the  $u_g(t)$  process, and  $Y(\omega)$  is the power spectrum corresponding to the stationary process  $y(t)$ .

Herein, the envelop function given by the equation (Bogdanoff et al. 1961)

$$A(t) = Ct \exp\left(\frac{-bt}{2}\right) \quad (3)$$

is adopted to account for the time-varying intensity observed in typical field recorded accelerograms pertaining to historic seismic events. In the above equation the parameter  $C$  is proportional to the intensity of the ground acceleration process. Furthermore, the parameter  $b$  specifies the width of the envelop function and, thus, it controls the duration of the ground motion. For instance, it can be shown that the parameter  $b$  is related to the “significant effective duration”  $T_{eff}$  defined by Trifunac and Brady (1975) as

$$T_{eff} = t_{95} - t_{05}, \quad (4)$$

by means of the following system of non-linear equations (Spanos et al. 2009)

$$\begin{cases} (b^2 t_{95}^2 + 2b t_{95} + 2) \exp(-b t_{95}) = 0.1 \\ (b^2 t_{05}^2 + 2b t_{05} + 2) \exp(-b t_{05}) = 1.9 \end{cases} \quad (5)$$

In Eqs. (4) and (5)  $t_{05}$  and  $t_{95}$  denote the time instants at which the 5% and the 95% of the total energy of the acceleration process has been released, respectively. Note that although numerous definitions for the duration of strong ground motion based on field recorded accelerograms have been proposed in the literature (see e.g. Bommer and Martinez-Pereira 1999, and references therein), the herein adopted one is commonly used by the structural engineering community (see e.g. Hancock and Bommer 2006).

For the purposes of this study commonly used for earthquake engineering applications stationary power spectra are considered in conjunction with Eq. (2), namely, the Kanai-Tajimi (K-T) spectrum given by the equation (Kanai 1957)

$$Y_{KT}(\omega) = \frac{1 + 4\zeta_g^2 \left(\frac{\omega}{\omega_g}\right)^2}{\left(1 - \left(\frac{\omega}{\omega_g}\right)^2\right)^2 + 4\zeta_g^2 \left(\frac{\omega}{\omega_g}\right)^2}, \quad (6)$$

and the Clough-Penzien (C-P) spectrum given by the equation (Clough and Penzien 1993)

$$Y_{CP}(\omega) = Y_{KT}(\omega) \frac{\left(\frac{\omega}{\omega_f}\right)^4}{\left(1 - \left(\frac{\omega}{\omega_f}\right)^2\right)^2 + 4\zeta_f^2 \left(\frac{\omega}{\omega_f}\right)^2}. \quad (7)$$

These phenomenological models account for the influence of the surface soil deposits on the frequency content of the propagating seismic waves via the “stiffness” ( $\omega_g$ ) and “damping” ( $\zeta_g$ ) parameters. The C-P spectrum incorporates an additional high-pass filter whose cut-off frequency and “steepness” are determined by the parameters  $\omega_f$  and  $\zeta_f$ . This filter suppresses the low frequencies allowed by the K-T spectrum: a quite desirable property to realistically capture the frequency content exhibited by field recorded strong ground motions. Further comments on the importance of selecting appropriately the spectral form of  $Y(\omega)$  appearing in Eq. (2) for the purposes of this study are included in section 5 in light of pertinent numerical results.

## **2.2. Formulation and solution of the inverse stochastic dynamics problem**

Consider a linear quiescent unit-mass single-degree-of-freedom (SDOF) system, with ratio of critical viscous damping  $\zeta_n$  and natural frequency  $\omega_n$ , base-excited by the acceleration process  $u_g(t)$ . The relative displacement response process  $x(t)$  of this system with respect to the motion of its base is governed by the equation

$$\ddot{x}(t) + 2\zeta_n\omega_n\dot{x}(t) + \omega_n^2x(t) = -u_g(t), \quad (8)$$

in which a dot over a symbol denotes time differentiation and zero initial conditions are assumed. Focusing on lightly damped systems (i.e.  $\zeta_n < 0.1$ ), the response  $x(t)$  is assumed to be a narrow-band process. In this case the time-evolving variance  $\sigma_x^2$  of the response process

$x(t)$  can be reliably approximated by the variance  $\sigma_a^2$  of its amplitude (e.g. Spanos 1978).

The latter quantity can be expressed by the following equation (Spanos and Lutes 1980)

$$\sigma_a^2(t, \omega_n, \zeta_n, G) = \frac{\pi}{\omega_n^2} \exp(-2\zeta_n \omega_n t) \int_0^t \exp(2\zeta_n \omega_n \tau) G(\tau, \omega_n) d\tau. \quad (9)$$

Given an EPS  $G$  the “forward” problem of deriving a relative displacement response spectrum  $S_d(\omega_n, \zeta_n, G)$  associated with this EPS can be formally expressed by the equation

$$S_d(\omega_n, \zeta_n, G) = \max_t \{ |x(t)| \}. \quad (10)$$

However, in the practice of aseismic design of structures often only a relative displacement elastic response spectrum  $S_d(\omega_n, \zeta_n)$  is provided to the designer for the definition of the input seismic severity. In relating the latter spectrum to an EPS  $G(t, \omega)$  defined by Eq. (2) an “inverse” stochastic dynamics problem must be considered. Following Spanos and Vargas Loli (1985), this problem can be formulated by relying on the equation (see also Giaralis and Spanos 2009)

$$S_d(\omega_n, \zeta_n) = r(\omega_n, \zeta_n, G, p) \max_t \{ \sigma_a(t, \omega_n, \zeta_n, G) \}. \quad (11)$$

In the above equation the so-called “peak factor”  $r$  is the critical parameter establishing the equivalence between the given response spectrum  $S_d$  and the EPS  $G$  to be determined in a statistical manner (see e.g. Vanmarcke 1976). The peak factor corresponds to the scalar by which one needs to multiply the peak standard deviation of the response amplitude (assumed to be equal to the peak standard deviation of the response process  $x$ ) attained at some time instant  $t_{max\ var}$  to reach a certain peak response level  $S_d$  with probability  $p$ . Thus, provided the variance  $\sigma_a^2$  in Eq. (9) can reliably approximate the variance of the response process  $x(t)$ , the achieved level of compatibility of the process  $u_g(t)$  with any given response spectrum relies significantly on the choice of the peak factor  $r$ . In case the given (target) spectrum is a

uniform hazard spectrum (UHS), as commonly prescribed by aseismic codes of practice, then  $S_d$  in Eq.(11) needs to be treated as the “median response spectrum”. In this respect, Eq. (11) establishes the following criterion: considering an ensemble of non-stationary samples compatible with  $G$  (i.e. generated as described in the following section 2.3), half of the population of their response spectra will lie below  $S_d$  (Vanmarcke 1976). To fulfill this criterion a “median” peak factor corresponding to  $p= 0.5$  needs to be considered which requires knowledge of the probabilistic structure of  $r$ . However, the peak factor is a quantity associated with the first passage problem of stochastically excited linear SDOF systems exposed to uniformly modulated input processes for which no closed solution exists. To this end, Monte Carlo simulations for input EPSs compatible with specific UHS are undertaken to define appropriate median peak factors to be used in the solution of Eq. (11). Further discussion on this issue is included in following sections in light of pertinent numerical results.

Once a specific value for the peak factor and a parametric form for the EPS  $G$  are assumed, an approximate point-wise solution of the inverse problem of Eq. (11) can be obtained by minimizing the error (Giaralis and Spanos 2009)

$$e = \sum_{j=1}^{2M} (S_j - q_j)^2, \quad (12)$$

at a certain set of  $M$  natural frequencies  $\{\omega_{n(j)}\}$  for  $j= 1, \dots, M$ . In the above equation the quantities  $S_j$  and  $q_j$  are given by the formulae

$$S_j = \begin{cases} S_d^2(\omega_{n(j)}, \zeta_n) & , \quad j = 1, \dots, M \\ 0 & , \quad j = M + 1, \dots, 2M \end{cases}, \quad (13)$$

and

$$q_j = \begin{cases} \frac{r^2 \pi C^2 t_j^{*2} \exp(-bt_j^*)}{2\zeta_n \omega_{n(j)}^3} Y(\omega_{n(j)}) & , \quad j = 1, \dots, M \\ \gamma_{j-M}^2 (2t_{j-M}^* - bt_{j-M}^{*2}) - 2\gamma_{j-M} (1 - bt_{j-M}^*) - \\ -2b + 4\zeta_n \omega_{n(j-M)} \exp(-\gamma_{j-M} t_{j-M}^*) & , \quad j = M + 1, \dots, 2M \end{cases} \quad (14)$$

respectively, where  $\gamma_j = 2\zeta_n \omega_{n(j)} - b$  and  $t_j^*$  is the time instant at which the variance  $\sigma_a^2(t)$  corresponding to the linear SDOF system with natural frequency  $\omega_{n(j)}$  is maximized. In all of the ensuing numerical results, a Levenberg-Marquardt algorithm with line search (see e.g. Nocedal and Wright 1999), implemented in the built-in function 'lsqcurvefit' available in MATLAB<sup>®</sup> is used to solve the set of  $2M$  non-linear equations defined by Eqs. (12)~(14). In this context, the herein considered inverse stochastic dynamics problem is treated as a nonlinear least-square fit optimization problem. The unknowns to be determined are the  $M$   $t_j^*$  time instants and the parameters involved in the definition of the EPS form: four in the case of the K-T spectrum ( $C, b, \omega_g, \zeta_g$ ) or six in the case of the C-P spectrum ( $C, b, \omega_g, \zeta_g, \omega_f, \zeta_f$ ). In a practical numerical implementation, the number of the frequencies  $M$  can always be set such that the aforementioned optimization problem is over-determined and thus readily solvable. Furthermore, it is pointed out that the parameter  $b$  can either be treated as an unknown “free” parameter to be determined by the optimization algorithm, or it can be held fixed at a predefined value corresponding to a specific effective duration. In this way, the optimization algorithm is “forced” to yield an EPS corresponding to a non-stationary process of specific duration. Additional comments along with numerical results on this issue are included in section 4.

### ***2.3. Spectrum compatible random field simulation for Monte Carlo analysis***

Upon determination of the parameters defining the EPS  $G$  as detailed in the previous section, one can employ a random field simulation technique to generate samples of the

underlying non-stationary process compatible with this EPS. These samples can be viewed as artificial acceleration time-histories (accelerograms). Such accelerograms can be numerically generated by first synthesizing stationary discrete-time signals as sampled versions of the continuous-time stochastic process  $y(t)$  appearing in Eq. (1). That is,

$$y[s] = y(sT_s) \quad , \quad s = 0, 1, \dots, N, \quad (15)$$

where  $T_s$  is the sampling interval which must be equal to, at least,  $\pi/\omega_b$  to avoid aliasing according to the well-known Nyquist criterion and  $N$  should be selected appropriately so that  $A(NT_s)$  attains a negligible non-zero value. Next, these stationary records are multiplied individually by the corresponding discrete/sampled version of the envelop function defined in Eq. (2) to obtain the final artificial records with non-stationary intensity as Eq. (1) suggests.

In this study, stationary discrete-time signals  $\tilde{y}[s]$  are synthesized by filtering arrays of discrete-time Gaussian white noise  $w[s]$  with a two-sided unit-intensity power spectrum band-limited to  $\omega_b$  through an autoregressive-moving-average (ARMA) filter of order  $(m, n)$ . In a practical numerical implementation setting these arrays comprise pseudo-random numbers belonging to a Gaussian distribution with zero mean and variance equal to  $\sqrt{2\omega_b}$ .

The aforementioned filtering operation is governed by the difference equation

$$\tilde{y}[s] = -\sum_{k=1}^m d_k \tilde{y}[s-k] + \sum_{l=0}^n c_l w[r-l], \quad (16)$$

in which  $c_l$  ( $l=0, 1, \dots, n$ ) and  $d_k$  ( $k= 1, \dots, m$ ) are the ARMA filter coefficients. Herein, the auto/cross-correlation matching (ACM) method is adopted to determine these coefficients so that the power spectrum of the process  $\tilde{y}[s]$  matches the CP spectrum  $Y(\omega)$  of the process  $y[s]$ . In this manner, the process  $\tilde{y}[s]$  can reliably model the process  $y[s]$ . The mathematical details of the ACM method can be found in Spanos and Zeldin (1998).

The time-histories generated as discussed above are further processed to address the issue of baseline correction. This is accomplished efficiently by appropriate zero-padding and forward/backward filtering of the records using a standard Butterworth high-pass filter of order 4 and cut-off frequency 0.10Hz (see e.g. Boore 2005, Giaralis and Spanos 2009).

It is noted, in passing, that the herein presented simulation technique is considered in the following sections solely for the purpose of deriving peak factors in a Monte Carlo based analyses and to assess the quality of compatibility achieved between the nonstationary processes represented by the considered EPSs with the given response spectrum. The simulation of individual samples is not part of the considered approach for deriving response spectrum compatible processes.

### **3. Application to the EC8 elastic design spectrum**

This section considers the elastic (uniform hazard) response spectrum prescribed by the European aseismic code provisions (EC8) (Eq. (A.1) of the Appendix A) as a paradigm to demonstrate that the consideration of frequency and damping dependent median peak factor spectra in the solution of the inverse stochastic formulation discussed in section 2.2 yield non-stationary processes achieving excellent compatibility with the target UHS. In all the numerical work of this section, the C-P spectral form given by Eq. (7) is considered in minimizing the error defined in Eq. (12). Furthermore, the  $b$  parameter involved in the definition of the envelop function in Eq. (3) is treated as a “free” parameter.

#### ***3.1. Peak factor estimation via Monte Carlo analysis***

As it has been already discussed in section 2.2, in case a UHS is set as the target spectrum, the desired level of compatibility between this spectrum and the sought stochastic process can be theoretically achieved by considering the median peak factor. Given that no dependable analytical expression is available for this quantity, comprehensive Monte Carlo-based analyses are conducted to derive natural frequency and damping dependent peak factors (peak factor spectra) for uniformly modulated C-P processes compatible with the EC8 response spectrum. Specifically, C-P evolutionary power spectra (EPSs) compatible with the EC8 spectrum for peak ground acceleration (PGA) of 0.36g ( $g= 9.81 \text{ m/sec}^2$ ), for three different damping ratios  $\zeta_n= 2\%$ , 5%, and 8% and for all five soil conditions prescribed by the EC8 are considered: a total of 15 EPSs. These have been obtained as discussed in section 2.2 assuming a constant peak factor  $r= (3\pi/4)^{1/2}$  (see also Giaralis and Spanos 2009). For each of the thus obtained EPSs a suite of 10000 spectrum-compatible non-stationary artificial accelerograms are generated and base-line adjusted as described in section 2.3. Next, each suite is “fed” to a series of 200 linear SDOF systems with natural periods ranging from 0.02s to 6s. The damping ratio of these systems is set to coincide with the value of  $\zeta_n$  considered in deriving each of the EPS from the corresponding EC8 spectrum. For every such system defined by the properties  $T_n= 2\pi/\omega_n$  and  $\zeta_n$  and excited by a specific suite of accelerograms the response ensembles ( $x^{(k)}(t)$ ;  $k=1,2,\dots,10000$ ) are calculated via numerical integration of Eq. (8) (Nigam and Jennings 1969). Finally, populations of peak factors ( $r^{(k)}$ ;  $k=1,2,\dots,10000$ ) are computed from the above ensembles as the ratio of the population of peak responses over the maximum averaged standard deviation of the response ensemble. That is,

$$r^{(k)}(T_n, \zeta_n, G) = \frac{\max_t \left\{ \left| x^{(k)}(t, T_n, \zeta_n, G) \right| \right\}}{\max_t \left\{ \sqrt{\text{mean}_k \left\{ \left( x^{(k)}(t, T_n, \zeta_n, G) \right)^2 \right\}} \right\}}. \quad (17)$$

It is important to note that these peak factor populations are independent of the intensity of the excitation. Thus, they are neither influenced by the adopted PGA value assumed in the derivation of the 15 considered EPSs nor by the adopted constant peak factor value  $r = (3\pi/4)^{1/2}$  involved in this derivation. However, they do reflect the different spectral contents and effective durations (as controlled by the  $b$  parameter of Eq. (3)) of the considered EPSs.

In the course of computing the denominator of Eq. (17) two quantities need to be considered. The first quantity is the peak value of the time-evolving mean square of the response ensembles. This value approximates numerically the peak variance  $\max\{\sigma_x^2\}$  since the simulated signals are base-line corrected to be zero-mean. The second quantity is the time  $t = t_{\max \text{ var}}$  at which this peak value is attained. Fig. 1 provides plots of both of these quantities as functions of the natural period of the SDOF systems considered for damping ratio  $\zeta_n = 5\%$  for the five EC8 soil types. The spectral shapes of the variance in Fig. 1(a) are comparable to the EC8 displacement response spectrum plotted in Fig. 12 of the Appendix. Moreover, as more flexible oscillators are considered the maximum response variance is reached at later times. Similar trends have been observed for the obtained data corresponding to  $\zeta_n = 2\%$  and  $8\%$ , not included here for brevity.

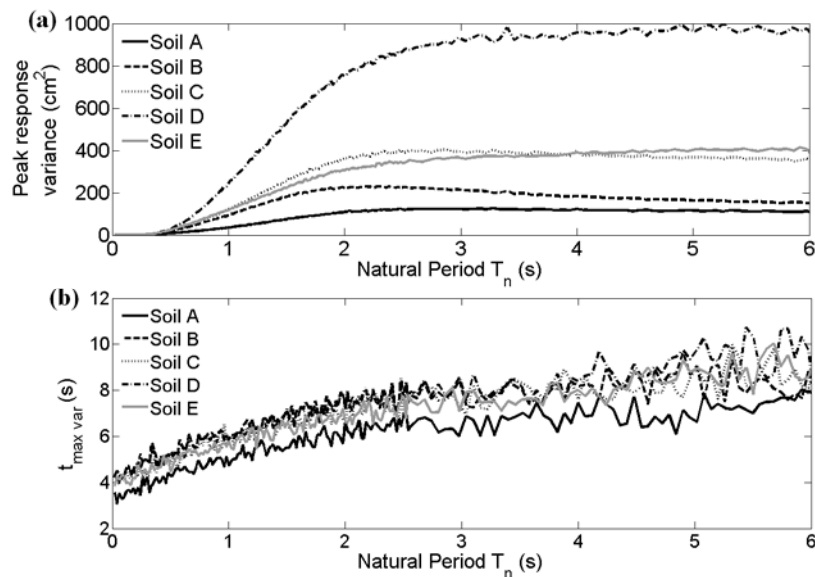


Fig. 1: Peak variances and time instants at which these peak values are attained for response ensembles pertaining to EC8 spectrum compatible EPSs for PGA= 0.36g and  $\zeta_n=5\%$ .

Note that in the solution of the stochastic dynamics problem of section 2.2 the variance of the response amplitude  $\sigma_a^2$  and the time  $t^*$  at which this is maximized have been considered instead of the corresponding  $\sigma_x^2$  and  $t_{\max \text{ var}}$  quantities, respectively. Fig. 2 provides indicative data to assess the validity of these considerations in view of the herein considered simulated data. In particular, Fig. 2(a)~(f) plots the time dependent response variances of various oscillators for input EPSs compatible with the EC8 spectrum for soil types B and C and for  $\zeta_n=5\%$ . The gray lines ( $\sigma_x^2(t)$ ) are obtained from the simulated response time-histories while the black lines are computed from the analytical expression

$$\sigma_a^2(t, \omega_n, \zeta) = \frac{\pi C^2}{\omega_n^2 \gamma^3} \left[ \gamma^2 t^2 \exp(-bt) - 2\gamma t \exp(-bt) + 2 \exp(-bt) - 2 \exp(-2\zeta \omega_n t) \right], \quad (18)$$

where  $\gamma = 2\zeta_n \omega_n - b$ . The latter expression is obtained by substitution of Eqs. (2) and (3) in Eq. (9). It is observed that better agreement between the simulated and the analytical data is achieved for stiffer oscillators. Still, the overall quality of the agreement is acceptable for the range of natural periods of practical interest for earthquake engineering applications. Similar conclusions are drawn by examining the data plotted in Fig. 2(g)~(k) pertaining to the aforementioned EC8 compatible EPSs. In the latter plots, the Monte Carlo-based results for soil B and C types included in Fig. 1(a) and Fig. 1(b) are compared with the peak response amplitude, given analytically by the equation

$$\max_t \{ \sigma_a^2(\omega_n, \zeta) \} = \sigma_a^2(t = t^*, \omega_n, \zeta) = \frac{\pi C^2 t^{*2} \exp(-bt^*)}{2\zeta \omega_n^3} S(\omega_n), \quad (19)$$

and with the time instants  $t^*$  satisfying the condition

$$\gamma^2(2t^* - bt^{*2}) - 2\gamma(1 - bt^*) - 2b + 4\zeta\omega_n \exp(-\gamma t^*) = 0, \quad (20)$$

respectively. The condition of Eq. (20) is reached by setting the first time derivative of Eq. (18) equal to zero, while Eq. (19) is derived by applying the above condition in Eq. (18) and by making use of Eqs. (2) and (3). Similar level of matching between simulated and analytical data as those observed in Fig. 2 is achieved for all 15 EC8 compatible EPSs considered in the undertaken Monte Carlo analyses. The good agreement between the simulated data with the corresponding analytical expressions confirms that the assumptions made in formulating the stochastic dynamics problem of section 2.2 are valid for the purposes of this work.

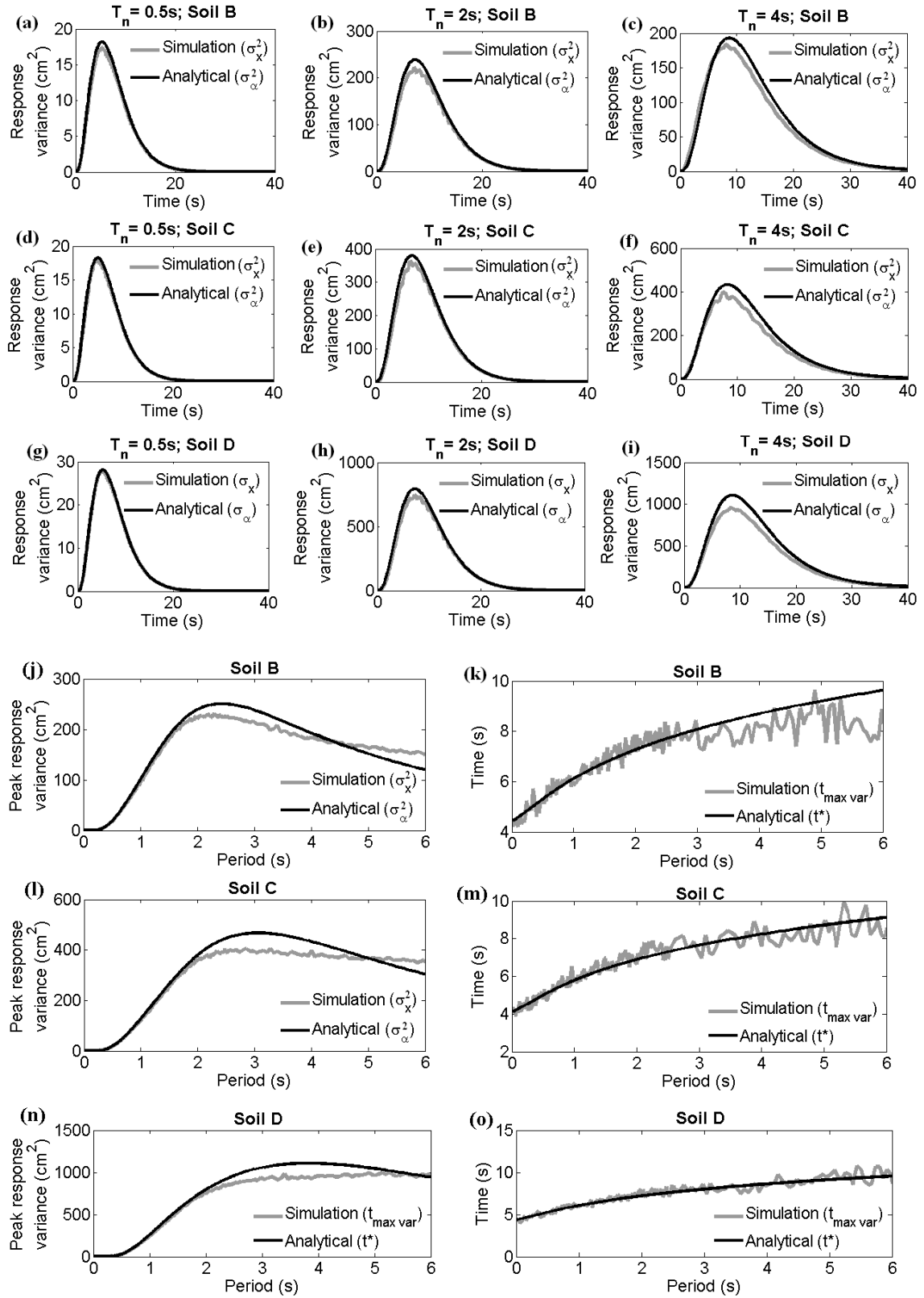


Fig. 2: Time-evolving response variances (panels (a)~(i)), peak response variances (panels (g) and (i)), and time instants at which these peak values are attained (panels (j) and (o)) of various oscillators for input EC8 compatible EPSs ( $PGA = 0.36g$ ;  $\zeta_n = 5\%$ ; Soils B, C and D).

Furthermore, the computation of the numerator in Eq. (17) involves the calculation of the time instants  $t_{max|x|}$  at which the peak value of each response time-history is attained. In Fig. 3, certain plots associated with the statistical properties of the  $t_{max|x|}$  populations normalized by the  $t_{max\ var}$  time instants for EC8 compatible input EPSs with  $\zeta_n=5\%$  are shown. Specifically, Fig. 3(a) and Fig. 3(b) plot the average and standard deviation, respectively, of these populations for all EC8 soil conditions as a function of natural period (mean and standard deviation spectra). The mean spectral values fluctuate around unity with small dispersion for all soil types, although a noticeable trend of linear decrease towards the longer periods exists. This result agrees with the intuition which suggests that the time instants at which the peak response and the peak response variance are obtained should be in a close agreement, on the average. Nevertheless, the standard deviation spectra reveal that there is a significant dispersion in the population of the samples (10000 for each oscillator). To further elucidate this point, six histograms of such populations related to certain oscillators and the corresponding fitted gamma distributions (solid lines) are included in Fig. 3. It was found that the gamma distribution yielded the best parametric fitting results based on a standard maximum likelihood estimation algorithm. Note that the gamma distribution of a positive valued random variable  $z$  reads

$$f(z / \kappa, \theta) = \frac{1}{\theta^\kappa \Gamma(\kappa)} z^{\kappa-1} \exp\left(-\frac{z}{\theta}\right), \quad (21)$$

where  $\Gamma(\cdot)$  denotes the standard gamma function and  $\kappa$ ,  $\theta$  are the “shape” and “scale” parameters, respectively. Similar results as those reported in Fig. 3 have been observed for response ensembles corresponding to  $\zeta_n=2\%$  and  $8\%$ .

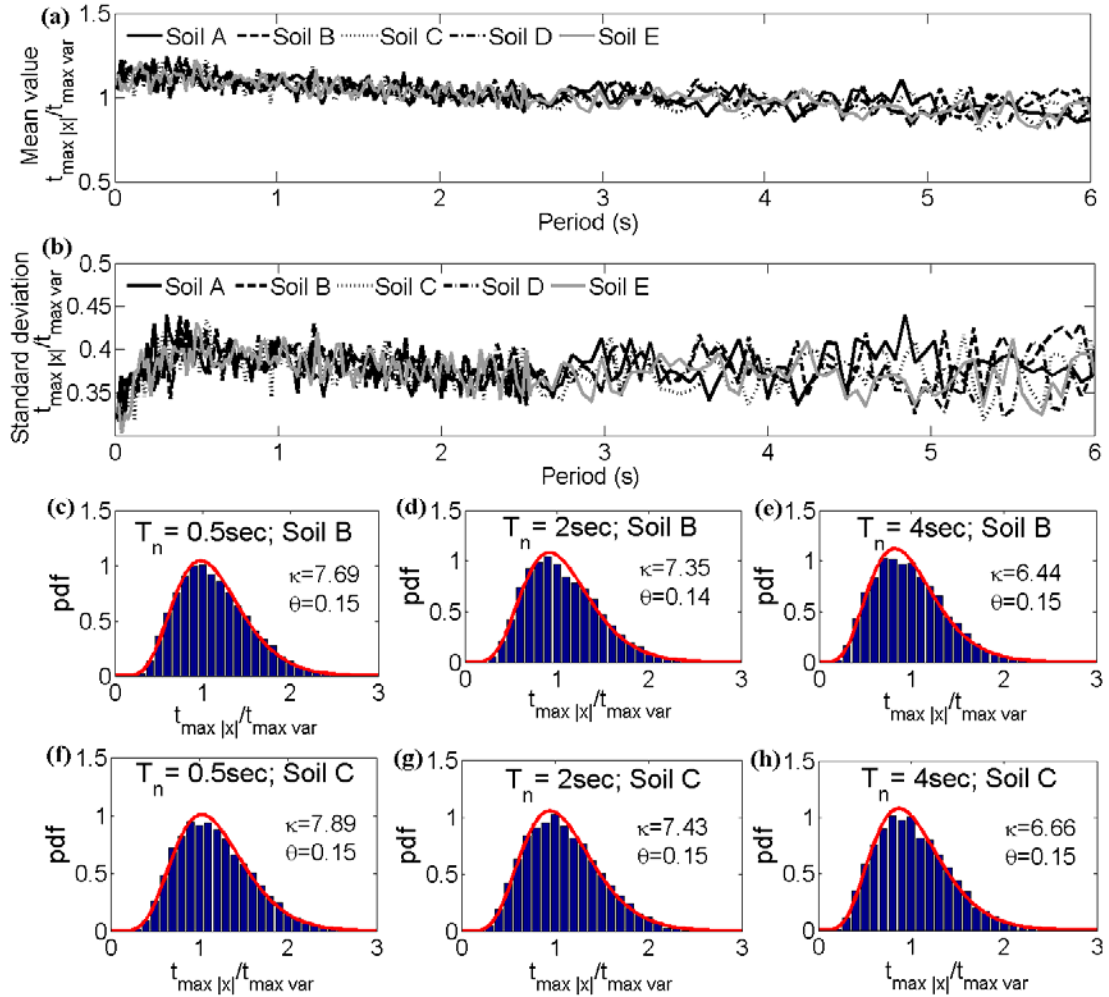


Fig. 3: Mean value spectra (panel (a)), standard deviation spectra (panel (b)), and histograms (panels (c)~(h)) of populations of ratios  $t_{\max |x|} / t_{\max \text{ var}}$  for response ensembles pertaining to EC8 spectrum compatible EPSs for PGA= 0.36g and  $\zeta_n= 5\%$ .

Similar statistical results as those presented in Fig. 3 are collected in Fig. 4 corresponding to peak factor populations calculated by Eq. (17). In particular, the median of the peak factors plotted against the natural period (median peak factor spectra) for all the EC8 soil conditions ( $\zeta_n= 5\%$ ) are shown in Fig. 4(a). Evidently, the median peak factor possesses a complicated dependence with the natural period of linear SDOF oscillators. Interestingly, similar trends have been previously reported in the literature (see e.g. Vanmarcke 1976). From a practical viewpoint, the most important conclusion drawn from Fig. 4(a) is that the

five curves lie very close to each other. This means that the various shapes of the EC8 spectrum corresponding to different soil conditions (Fig. 12 in the appendix) reflecting on the considered EPSs have a minor effect on the median peak factor spectrum (see also Spanos et al. 2009). This fact facilitates significantly the derivation of EPSs compatible with the EC8 spectrum in the average statistical sense as discussed in the next sub-section. Note that this observation is valid when treating  $b$  as a “free” parameter in deriving the EC8 compatible EPSs. The case where  $b$  is predefined to yield processes of a pre-selected effective duration is discussed in section 4.

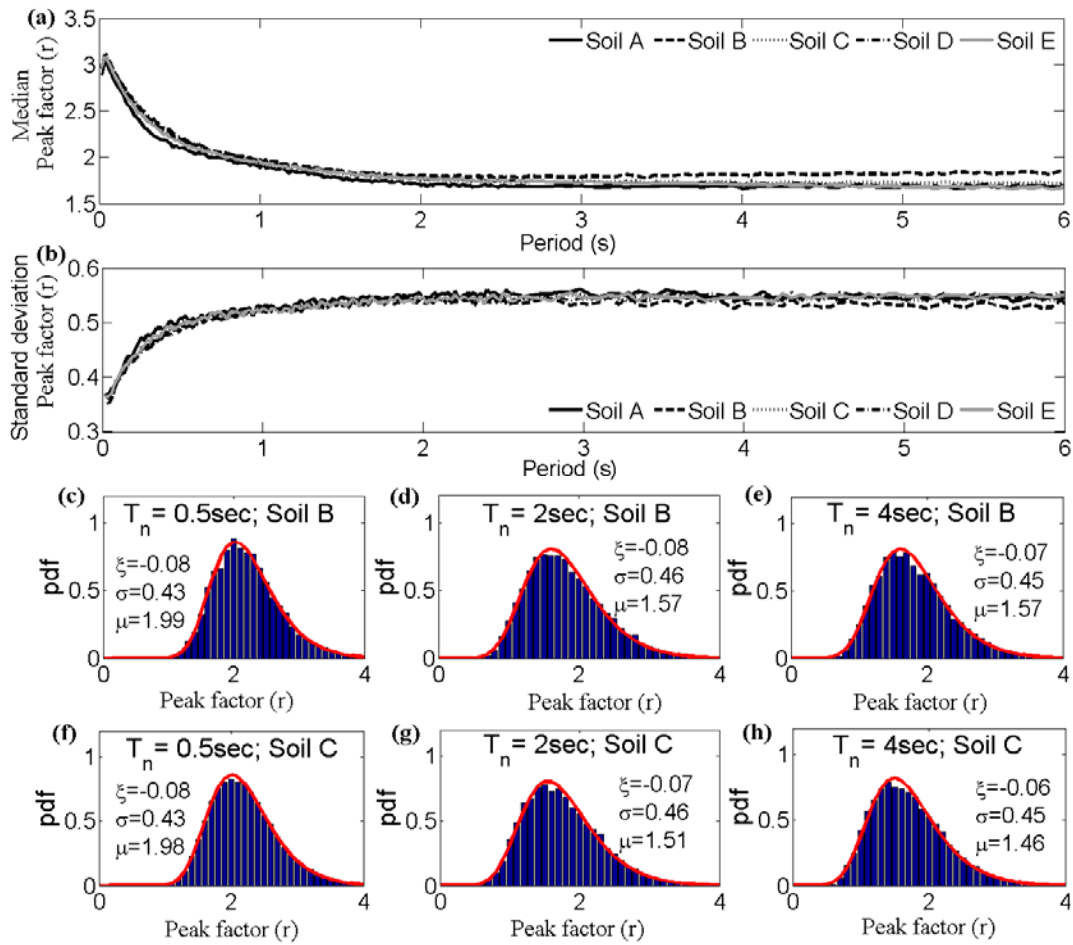


Fig. 4: Median spectra (panel (a)), standard deviation spectra (panel (b)), and histograms (panels (c)~(h)) of populations of ratios  $t_{max|x|} / t_{max var}$  for response ensembles pertaining to EC8 spectrum compatible EPSs for  $PGA = 0.36g$  and  $\zeta_n = 5\%$ .

Focusing on the standard deviation of the peak factor populations shown in Fig. 4(b) it is noted that it is certainly non-negligible and that it varies for natural periods up to 1s approximately. For higher periods, it practically attains a constant value. For the sake of completeness, histograms of peak factor populations have been also included in Fig. 4 related to the same oscillators and input EPSs as in Fig. 3. Generalized extreme value distributions given by the equation

$$f(z/\xi, \sigma, \mu) = \frac{1}{\sigma} \exp\left(-\left(1 + \xi \frac{z - \mu}{\sigma}\right)^{-1/\xi}\right) \left(1 + \xi \frac{z - \mu}{\sigma}\right)^{-1-1/\xi} \quad (22)$$

have been fitted to these histograms (solid lines). In the above equation  $\mu$  corresponds to the “center of mass” of the population,  $\sigma$  is a “spread” factor and  $\xi$  is the “shape” factor, while the expression inside the parenthesis is always positive. Note that in all cases examined the value of parameter  $\xi$  is negative. This corresponds to a “type III” extreme value distribution of the Weibull kind (e.g. Kotz and Nadarajah 2000). It is further reported that similar statistical analyses of the peak factor populations of the response ensembles for EPSs corresponding to  $\zeta_n=2\%$  and  $8\%$  has yielded the same observations and conclusions as those for  $\zeta_n=5\%$ . Thus, the inclusion of numerical results from these analyses has not been deemed essential.

### ***3.2. EC8 compatible median peak factor and evolutionary power spectra***

As it has been already alluded in the paper, median peak factor spectra are required to be used in the herein adopted formulation for the purpose of deriving non-stationary processes compatible with a response spectrum in the mean sense. Notably, as discussed in the previous sub-section, the median peak factor spectra computed from ensembles of EC8 spectrum compatible EPSs are relatively insensitive to the shape attained by the EC8

spectrum for different soil conditions. Therefore, it is reasonable to consider the average of the median peak factor spectra for the various soil conditions of EC8 for each value of the damping ratio herein considered. Further, polynomial curve fitting is applied to the above averaged median peak factor spectra to obtain an analytical expression to approximate the numerically derived median peak factors. The 8<sup>th</sup>-order polynomials plotted in Fig. 5 and expressed by the equation for  $Q=8$

$$\hat{r}(T) = \sum_{j=0}^Q p_j T^j, \quad 0.02 \leq T \leq 6 \text{ sec} \quad (23)$$

approximate reasonably well the averaged median peak factor spectra for periods up to 6s. The coefficients  $p_j$  of these polynomials are given in Table 1. For oscillators of natural periods longer than 6s a constant peak factor of  $r = \hat{r}(6)$  can be utilized.

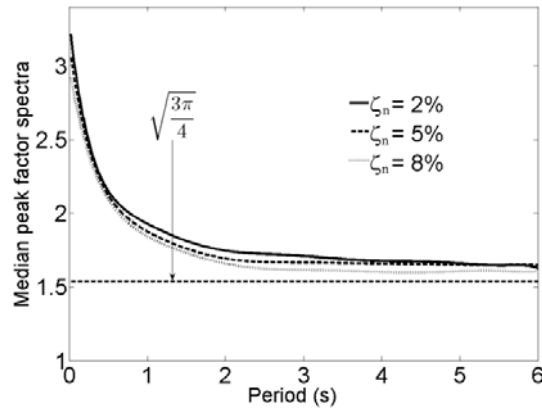


Fig. 5: Polynomial fit to EC8 compatible median peak factor spectra for various levels of damping  $\zeta_n$ .

Table 1: Coefficients of the fitted polynomials to the averaged numerically obtained median peak factor spectra of Fig. 5.

	<b>P<sub>0</sub></b>	<b>P<sub>1</sub></b>	<b>P<sub>2</sub></b>	<b>P<sub>3</sub></b>	<b>P<sub>4</sub></b>	<b>P<sub>5</sub></b>	<b>P<sub>6</sub></b>	<b>P<sub>7</sub></b>	<b>P<sub>8</sub></b>
$\zeta_n = 2\%$	3.3079	-4.9375	8.3621	-8.3368	5.0420	-1.8983	0.4469	-0.0639	0.0051
$\zeta_n = 5\%$	3.1439	-3.9836	5.9247	-5.3470	2.9794	-1.0439	0.2305	-0.0311	0.0023
$\zeta_n = 8\%$	2.9806	-3.2070	4.1190	-3.1733	1.4746	-0.4144	0.0689	-0.0062	0.0002

Table 2 reports the parameters defining C-P EPSs compatible with the EC8 spectrum for PGA= 0.36g, damping ratio 5%, and for all soil conditions obtained by minimizing the error of Eq. (12) using the frequency-dependent averaged median peak factor spectrum  $\hat{r}$  of Eq. (23) for  $\zeta_n= 5\%$ . Moreover, in Fig. 6 median pseudo-acceleration response spectra for ensembles of 100 baseline-corrected artificial accelerograms compatible with the C-P spectra of Table 2 for soil types B and C are plotted along with the corresponding (target) EC8 spectrum. Furthermore, the average, largest, and smallest spectral ordinates are also included to demonstrate the statistical nature of the considered data. Evidently, a satisfactory matching of the average response spectra of the generated signals with the target spectrum is attained which is in alignment with the compatibility criterion of Eq. (11) for  $p= 0.5$ . To demonstrate the influence of adopting appropriate values for the peak factor to achieve an acceptable level of matching as defined above, average pseudo-acceleration response spectra for ensembles of 100 baseline-corrected artificial accelerograms compatible with C-P EPSs derived by assuming a constant peak factor equal to  $(3\pi/4)^{1/2}$ , are superimposed in Fig. 6. Clearly, the use of the non-constant frequency dependent peak factors derived by the Monte Carlo analyses discussed in the previous sub-section improves significantly the quality of the pursued average matching compared to that achieved via a constant peak factor as previously considered in Giaralis and Spanos (2009). The significant discrepancy of the average response spectra obtained under the assumption of a constant peak factor  $(3\pi/4)^{1/2}$  from the target EC8 spectrum can be readily justified by considering the deviation of the averaged median peak factor spectrum from the constant level of  $(3\pi/4)^{1/2}$  shown in Fig. 5.

Table 2: Parameters for the definition of C-P evolutionary power spectra compatible with various EC8 spectra ( $\zeta_n = 5\%$ ) using the median peak factor spectra of Eq. (23)

Peak ground acceleration	Soil type	CP power spectrum parameters [ $T_{min} = 0.02, T_{max} = 10$ ] (s)					
		$C$ (cm/sec <sup>2.5</sup> )	$b$ (1/sec)	$\zeta_g$	$\omega_g$ (rad/sec)	$\zeta_f$	$\omega_f$ (rad/sec)
$\alpha_g = 0.36g$ ( $g = 981$ cm/sec <sup>2</sup> )	A	8.08	0.47	0.54	17.57	0.78	2.22
	B	17.76	0.58	0.78	10.73	0.90	2.33
	C	19.58	0.50	0.84	7.49	1.15	2.14
	D	30.47	0.50	0.88	5.34	1.17	2.12
	E	20.33	0.55	0.77	10.76	1.07	2.03

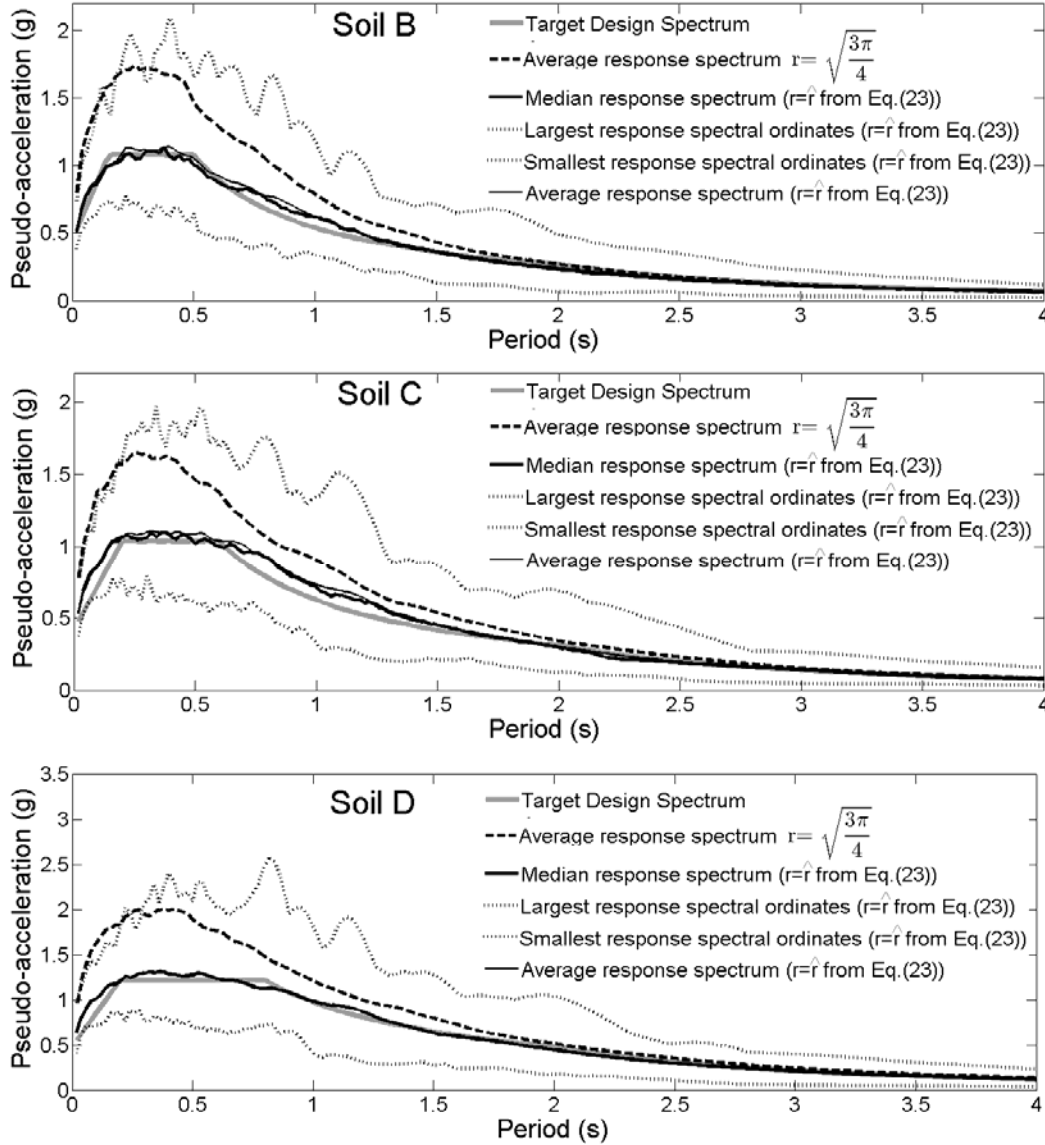


Fig. 6: Pseudo-acceleration response spectra of ensembles of 100 simulated accelerograms compatible with C-P evolutionary power spectra derived by assuming a constant peak factor of  $(3\pi/4)^{1/2}$  and the frequency-dependent peak factor of Eq. (23).

#### 4. Derivation of response spectrum compatible processes of specific effective duration

In this section the applicability of the stochastic formulation reviewed in section 2.2 to yield response spectrum compatible non-stationary processes of a prescribed effective duration ( $T_{eff}$ ) as defined by Trifunac and Brady (1975) is assessed. This is accomplished by utilizing the one-to-one relation established by Eqs. (4) and (5) between  $T_{eff}$  and the  $b$  parameter appearing in Eq. (3). The latter parameter is then treated as a constant in solving the inverse stochastic dynamics problem as detailed in section 2.2. The elastic response spectrum prescribed in the current aseismic code provisions effective in China (GB 50011 2001) for a fixed 5% ratio of critical damping is used as a paradigm of a target response spectrum (Eq. (A.2) of the Appendix). The K-T spectral form of Eq. (6) is assumed in the definition of the sought response spectrum compatible EPS (see also Spanos et al. 2009).

Similar Monte Carlo analysis, as discussed in the previous section, is conducted to estimate median peak factor spectra to achieve enhanced agreement between the target GB 50011 spectrum and the average response spectrum of populations of EPS compatible accelerograms. To this aim, K-T evolutionary power spectra (EPSs) compatible with the GB 50011 spectrum, for three different values of the  $b$  parameter, and for all the 14 values of the characteristic period  $T_g$  as prescribed in GB 50011 (see also Eq. (A.3) of the Appendix A) are considered: a total of 42 EPSs. These spectra have been derived by assuming a constant value for the peak factor while the  $b$  parameter has been taken equal to  $0.30s^{-1}$ ,  $0.40s^{-1}$ , and  $0.50s^{-1}$  corresponding to effective durations of approximately 18s, 14s, and 11s, respectively.

The thin black lines shown in Fig. 7 are the median peak factor spectra corresponding to the considered 42 GB 50011 compatible K-T EPSs. These spectra have been obtained from peak factor populations computed by Eq. (17) following the same procedure used to derive the spectra shown in Fig. 4a. That is, response time-history ensembles of 200 oscillators with different natural periods between 0.02s and 6s ( $\zeta_n$  is now fixed to 5%) have been utilized.

These oscillators have been driven by suites of 10000 accelerograms, each suite being compatible with a certain GB 50011 compatible K-T EPS. Notably, the thus derived median peak factor spectra corresponding to the same value of the  $b$  parameter (i.e. to the same effective duration) are closely clustered together. This suggests that the effective duration of the considered non-stationary uniformly modulated processes has a non-negligible influence on the peak factors: longer duration yields higher peak factor values. This observation is in alignment with what has been found for the case of finite-duration stationary processes (i.e. stationary processes modulated in the time-domain by a rectangular window), by various researchers (e.g. Vanmarcke 1976, Zembaty 1998, Sarkani et al. 2001). Furthermore, the aforementioned “clustering” of the median peak factor spectra suggests that the variation of the spectral content of the considered processes reflecting the different shapes of the GB 50011 spectrum dependent on the  $T_g$  (see Fig. 12 of the Appendix), has a minor effect on the peak factor values. Importantly, this has been the case for the median peak factor spectra compatible with the different shapes of the EC8 spectrum as well (see Fig. 4a). Thus, following a similar reasoning as in section 3.2, it is of practical interest to consider the average of the median GB 50011 compatible peak factor spectra for each value of the  $b$  parameter and to fit polynomial curves. In this manner, approximate analytical expressions for median GB 50011 compatible peak factor spectra corresponding to specific effective durations of the underlying strong ground motion are reached. Acceptable fit to the average of the considered median peak factor spectra is achieved by 7<sup>th</sup>-order polynomials expressed by Eq.(23) for  $Q=7$  and plotted in Fig. 7: The coefficients of these polynomials are reported in Table 3.

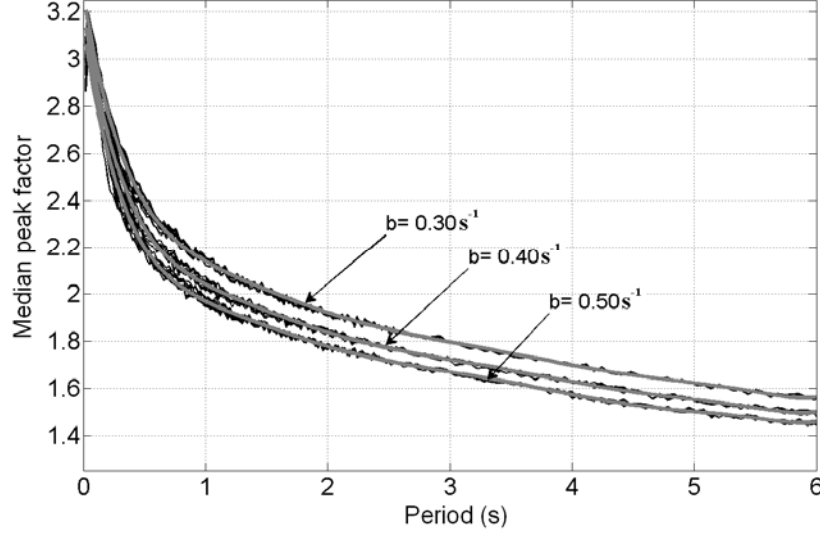


Fig. 7: Median peak factor spectra compatible with the GB 50011 spectrum (thin black lines) and fitted average median peak factor spectra given by Eq. (23) for  $Q=7$  (thick gray lines), for various values of the  $b$  parameter.

Table 3: Coefficients of the fitted polynomials to the averaged numerically obtained median peak factor spectra of Fig. 7.

	$p_0$	$p_1$	$p_2$	$p_3$	$p_4$	$p_5$	$p_6$	$p_7$
$b=0.30s^{-1}$ ( $T_{eff} \approx 18s$ )	3.2452	-2.8625	3.1451	-1.9687	0.7003	-0.1404	0.0148	-0.0006
$b=0.40s^{-1}$ ( $T_{eff} \approx 14s$ )	3.1711	-3.0196	3.4074	-2.1573	0.7724	-0.1556	0.0164	-0.0007
$b=0.50s^{-1}$ ( $T_{eff} \approx 11s$ )	3.1012	-3.1086	3.5941	-2.3085	0.8361	-0.1702	0.0181	-0.0008

Table 4 includes K-T EPSs compatible with the GB 50011 spectrum for  $\alpha_{max}=1.20g$  and  $T_g=0.70s$  corresponding to two different effective durations. These spectra have been derived by minimizing the error defined in Eq. (12) treating the  $b$  parameter as a constant and using the fitted average median peak factor spectra shown in Fig. 7: for  $b=0.30s^{-1}$  and  $b=0.50s^{-1}$ , respectively. As expected, the value of the  $C$  parameter related to the amplitude of the adopted envelop function (Eq. (3)) is significantly larger for the EPS corresponding to the  $b=0.50s^{-1}$  due to the reduced duration of the underlying non-stationary process compared to the  $b=0.30s^{-1}$  case. However, the  $\zeta_g$  and  $\omega_g$  parameters associated with the spectral content of the two non-stationary processes considered do not change significantly. In Fig. 8 average

pseudo-acceleration response spectra for ensembles of 500 baseline-corrected artificial accelerograms compatible with the EPSs of Table 4 are plotted along with the GB 50011 target spectrum. These average response spectra lie close to each other indicating that the two non-stationary processes, though of significantly different effective duration, are consistent in terms of peak response accelerations. To further illustrate this point arbitrarily chosen individual realizations compatible with the aforementioned EPSs are also included in Fig. 8 along with their response spectrum.

Table 4. K-T evolutionary power spectra compatible with the GB 50011-2001 design spectrum ( $T_g=0.70s$ ;  $\alpha_{max}= 1.20g$ ) for specific effective durations.

EPS Parameter (units)	( $b=0.30s^{-1}$ ) $T_{eff}\approx 18s$	( $b=0.50s^{-1}$ ) $T_{eff}\approx 11s$
$C(cm/s^{2.5})$	11.33	21.11
$b(1/s)$	0.30	0.50
$\zeta_g$	0.83	0.88
$\omega_g(rad/s)$	7.89	7.57

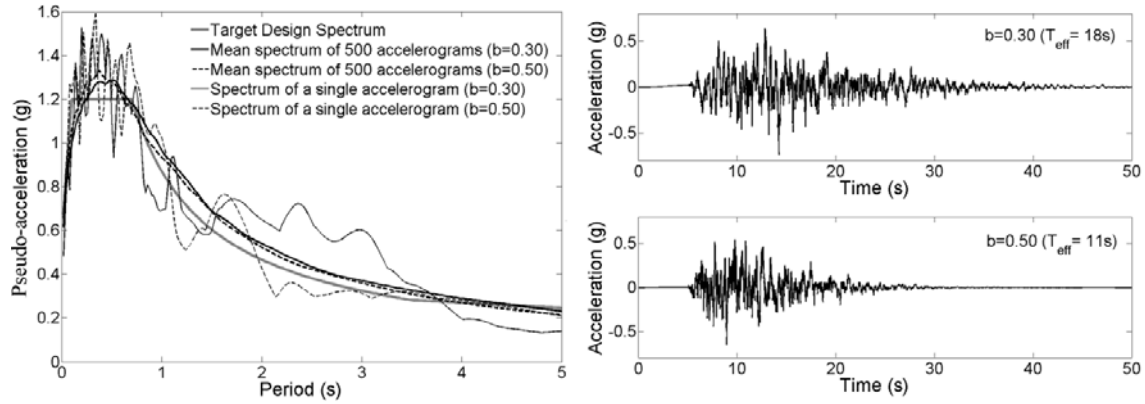


Fig. 8: Response spectra and time-histories of accelerograms of different effective durations compatible with the K-T evolutionary power spectra of Table 4.

Moreover, it is noted that both the average response spectrum curves included in Fig. 8 are in a close agreement with the target design spectrum. Similar results, not included here for brevity, have been obtained for other GB 50011 shapes and values of effective duration. In this regard, it can be argued that the EPSs derived by solving the herein adopted inverse

stochastic dynamics problem discussed in section 2.2 in conjunction with appropriately derived duration-dependent peak factor spectra can be used for structural aseismic design scenarios mandating the consideration of strong ground motions of specific duration (see e.g. Hancock and Bommer 2007).

## 5. Selection of the frequency content of the evolutionary power spectrum

In previous sections the influence of the peak factor and of the width of the envelop function of Eq.(3) in deriving response spectrum compatible non-stationary processes by minimizing the error in Eq. (12) has been addressed. However, the feasibility of achieving a numerical solution to this optimization problem relies further on choosing an appropriate parametrically defined spectral form for the stationary power spectrum  $Y(\omega)$  in Eq. (2). In particular, it appears that this choice depends on the behavior of the target response spectrum in the range of long periods (Giaralis and Spanos 2009). In fact, this is the reason why in the previous sections different parametric forms for  $Y(\omega)$ , namely the C-P (Eq. (7)) and the K-T (Eq. (6)), have been *a priori* considered to “fit” the considered EC8 and GB 50011 response spectra, respectively.

To further discuss this point, the EC8 spectrum for  $\alpha_g=0.25g$  and soil conditions B (see Eq. (A.1) of the Appendix) and the GB 50011 spectrum for  $\alpha_{max}=1.20g$  and  $T_g=0.40g$  (see Eq. (A.2) of the Appendix) are considered for comparison ( $\zeta_n=5\%$ ). These two target spectra are plotted in Fig. 9 in terms of pseudo-acceleration and relative displacement spectral ordinates. It is seen that they are characterized by radically different behavior for periods longer than  $T>2s$ . Specifically, the GB 50011 relative displacement spectrum increases monotonically for  $T>5T_g= 2s$ . This is because GB 50011 poses rather conservative (high) demands in terms of structural strength for flexible structures by prescribing a slow (linear) rate of decay to the last segment of the pseudo-acceleration spectral ordinates defined for

$T > 5T_g$  in Eq. (A.2). Arguably, the main reason for this consideration is to account for the contribution of higher modes which become important for flexible structures (e.g. mid-to-high-rise buildings), in the context of simplified response spectrum-based kinds of analysis relying considering only the first (fundamental) mode of vibration (e.g. Newmark and Hall 1982). However, this definition of the response spectrum does not comply with the theory of structural dynamics suggesting that the maximum deformation of very flexible seismically-excited SDOF oscillators is equal to the peak ground displacement (e.g. Chopra 2001). Consequently, it poses certain numerical difficulties in solving the inverse dynamics problem discussed in section 2.2. These difficulties are partly circumvented by adopting a spectral form  $Y(\omega)$  rich in low frequencies. The K-T spectrum of Eq. (6) defines such a spectral form and has been successfully used in the previous section as a mathematical instrument to accommodate the GB 50011 spectrum within the context of the herein adopted formulation. Note, however, that the low-frequency content allowed by the K-T spectrum is regarded as “spurious” as it is not in alignment with what is observed in field recorded accelerograms.

Nevertheless, the response spectrum of the EC8 is characterized by a behavior in the range of long periods which captures better the physics of the underlying structural dynamics problem (e.g. Faccioli et al. 2004). In fact, the EC8 pseudo-acceleration spectrum drops at an exponential rate for  $T > 2s$  in such a manner so that the corresponding relative displacement spectrum attains a constant value for very flexible oscillators. This attribute allows for utilizing phenomenological models to represent more realistically the low-frequency content of the strong ground motion than the K-T spectrum, such as the C-P spectrum given by Eq. (7).

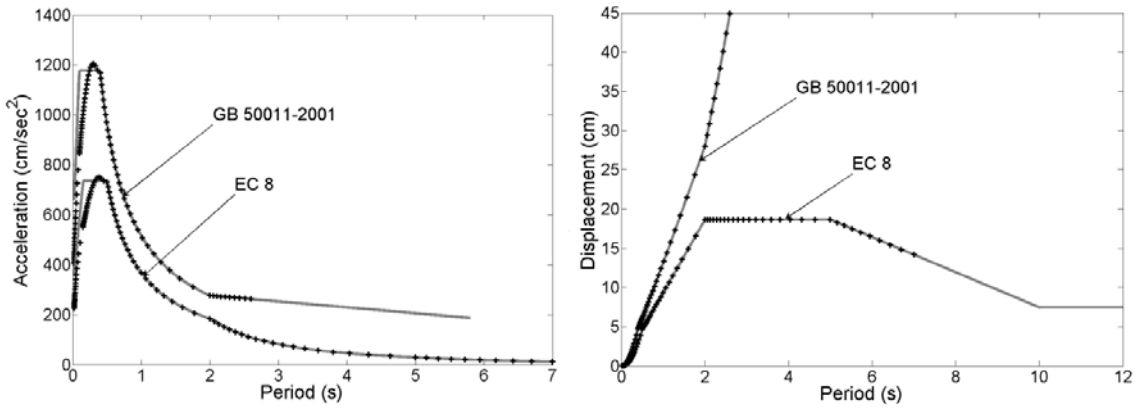


Fig. 9: EC8 ( $\alpha_g=0.25g$ ; soil B) and GB 50011 ( $\alpha_{max}=1.20g$ ;  $T_g=0.40g$ ) response spectra and point-wise least square matching.

Pertinent numerical results are included in support of the aforementioned comments illustrating the applicability of the adopted methodology to derive EPSs compatible with the considered response spectra. To this aim, Table 5 presents a K-T EPS and a C-P EPS compatible with the GB 50011 and the EC8 spectra plotted in Fig. 9. These EPSs have been derived by minimizing Eq. (13) treating  $b$  as a “free” unknown parameter and using the median peak factor spectra plotted in Fig. 10. The latter spectra have been derived as detailed in the previous sections. The quality of the point-wise matching achieved in solving the optimization problem is depicted via the dots included in Fig. 9 (see also Giaralis and Spanos 2009 and Spanos et al. 2009). These points correspond to the set of  $\{\omega_{n(j)}\}$  considered in Eqs. (13) and (14). As it has been previously reported in Spanos et al. (2009) if point-wise matching is pursued to include values of  $\omega_{n(j)}$  for periods beyond  $6.5T_g$  in the GB 50011 case the optimization algorithm fails to converge to an acceptable solution. This is due to the aforementioned behavior of the GB 50011 relative displacement spectra which does not converge to a constant value. However, in the EC8 case, the assumed C-P spectral form is able to trace the target spectrum in a point-wise manner to much higher natural periods.

Table 5. Evolutionary power spectra compatible with the target spectra of Fig. 9.

EPS Parameter (units)	C-P (EC8) (soil B; $\alpha_g=0.25g$ )	K-T (GB 50011) ( $T_g=0.40g; \alpha_{max}=1.20g$ )
$C(\text{cm/s}^{2.5})$	10.16	17.37
$b(1/s)$	0.54	0.50
$\zeta_g$	0.65	0.72
$\omega_g(\text{rad/s})$	12.76	15.67
$\zeta_f$	0.85	-
$\omega_f(\text{rad/s})$	2.15	-

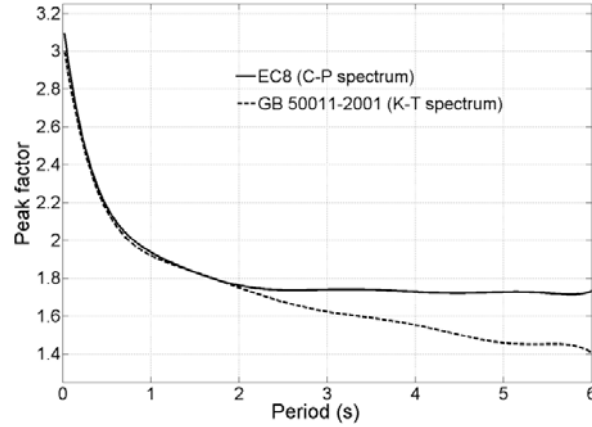


Fig. 10: Median peak factor spectra for  $\zeta=5\%$  compatible with the EC8 and the GB 50011 response spectra.

Interestingly, the differences in the frequency content of the assumed spectral forms (C-P and K-T) to accommodate the different target response spectra further influence the shape of the corresponding median peak factor spectra. This is seen in Fig. 10: the median peak factor spectra corresponding to C-P and K-T spectral forms coincide for periods up to 2s. For longer periods the EC8 compatible peak factors attain a constant value, while the GB 50011 peak factor spectrum is monotonically decreasing.

Finally, in Fig. 10 statistics of response spectra of 500 accelerograms compatible with the K-T and the C-P EPSs of Table 5, are compared with the respective target spectra. In both cases, enhanced agreement between the average response spectrum and the target spectrum for periods up to about  $5T_g=2s$  is achieved. For the C-P spectrum compatible accelerograms the quality of this agreement remains the same for  $T>2s$  which is not the case for the K-T

compatible accelerograms whose average spectral ordinates fall short of the GB 50011 spectrum. This result confirms numerically that the GB 50011 code poses rather high demands on flexible structures that even the K-T spectrum cannot accommodate in the region of periods higher than  $5T_g$  defining the corner period at which the last branch with the rather steep inclination of the target GB 50011 spectrum shown in Fig. 9 begins. As a final remark, it is noted that, if desired, spectral matching of the generated accelerograms in the  $T > 5T_g$  region can be accomplished by treating each sample separately using the various spectral matching approaches found in the literature (see e.g. Giaralis and Spanos 2009 and references therein). A frequency domain approach relying on the harmonic wavelet transform has been applied for this purpose in Spanos et al. (2009) to treat both artificial and field recorded accelerograms. However, it can be argued that such long fundamental periods are expected to be exhibited by “special” structures (e.g. base isolated buildings, long-span bridges etc.). The design of such structures would most probably involve considering site-specific response spectra and/or carefully selected field recorded accelerograms, rather than the uniform hazard code-specific spectra considered herein.

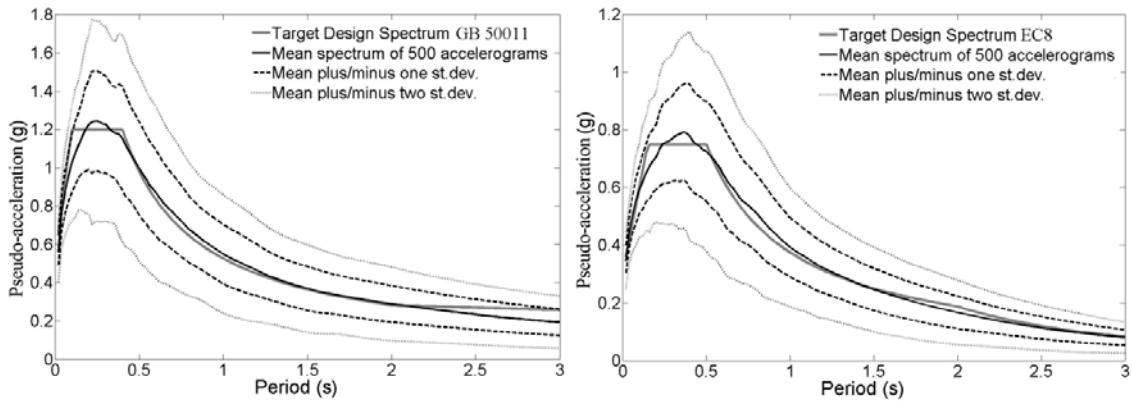


Fig. 11: Statistics of response spectra of an ensemble of 500 simulated accelerograms compatible with the EC8 and the GB 50011-2001 spectra of Fig. 9.

## 6. Concluding remarks

A non-iterative “one-step” methodology has been proposed to derive uniformly modulated stochastic processes compatible in the mean sense with a given (target) response (uniform hazard) spectrum (UHS) as commonly desired in the aseismic structural design regulated by contemporary codes of practice. This is accomplished by solving an established in the literature (Giaralis and Spanos 2009) inverse stochastic dynamics problem in conjunction with median peak factor spectra numerically derived by pertinent Monte Carlo analyses. The adopted solution “fits” directly to the target UHS simple, and thus attractive from a practical viewpoint, parametrically defined evolutionary power spectra (EPSs) characterizing the sought processes. The level of compatibility achieved is such that no additional treatment of the thus derived EPSs or of generated samples of the underlying processes need to be further considered. In this respect, the herein proposed methodology offers a novel straightforward approach to address the problem at hand as opposed to the usual “two-step” approach considered by various researchers in the past which involves the treatment of samples on an individual deterministic context (e.g. Gupta and Joshi 1993, Shrikhade and Gupta 1996, Crespi et al. 2002, Martinelli et al. 2011).

The applicability and usefulness of the proposed approach has been demonstrated by furnishing extensive numerical results pertaining to the European EC8 UHS (CEN 2004) and to the Chinese GB 50011 UHS. Special attention has been given on three important elements that need to be considered for the successful implementation of the adopted approach. These are a) the peak factor which governs the statistical nature of compatibility of the EPS with the considered UHSs, b) the shape of the envelop function which is associated with the effective duration of the sought stochastic processes, and c) the assumed frequency content of the parametric EPSs which needs to be appropriately pre-specified taking into account the asymptotic behavior of the target UHS for increasing natural periods.

Specifically, using the EC8 spectrum as a paradigm, and assuming a modulated Clough-Penzien (C-P) type of EPS, Monte Carlo analyses have been conducted to estimate numerically median peak factor spectra pertaining to all soil conditions defined in EC8 and to various damping levels. This need has been dictated by the fact that no convenient expression of the peak factor for the non-stationary input processes considered herein exists in the open literature to be used in the context of the adopted formulation. Additional numerical data derived as by-products of the above analysis have been also reported to elucidate certain aspects of the response of linear SDOF oscillators driven by uniformly modulated colored noise processes. Polynomial expressions have been fitted to the thus derived median peak factor spectra and the polynomial coefficients have been reported in a tabular form. These expressions have been further incorporated in the solution of the adopted inverse stochastic problem to yield EC8 consistent EPSs. The achieved level of consistency has been assessed by comparing the average and median populations of response spectra of large ensembles of EPS compatible artificial accelerograms. Compared with similar data incorporating a constant peak factor in the derivation of EC8 compatible EPSs (Giaralis and Spanos 2009) the average response spectra of the herein generated signals lie significantly closer to the EC8 spectrum. This result establishes the usefulness and practical merit of the reported EC8 compatible median peak factor and evolutionary power spectra to be used in the context of structural design regulated by the EC8 (see e.g. Giaralis and Spanos 2010, Martinelli et al. 2011). Incidentally, it is noted that the shapes of the EC8 spectrum for the various soil types exhibit considerable variations. Thus, it is reasonable to argue that the average EC8 median peak factor spectra herein derived may yield EPSs achieving close compatibility with any design spectra provided these can be captured by uniformly modulated C-P EPSs. Obviously, the latter argument warrants further numerical investigation.

Furthermore, numerical results pertaining to the GB 50011 design spectrum have been furnished to point out the fact that the adopted formulation is capable of deriving response spectrum compatible EPSs characterized by a prescribed “effective duration” as defined by Trifunac and Brady (1975). This has been accomplished by assigning appropriate values to the parameter controlling the width of the envelop function used in the definition of the EPSs. Further, Monte Carlo simulations have been carried out to numerically derive polynomial expressions of median peak factor spectra for various effective durations consistent with the GB 50011 design spectrum. These spectra have been incorporated in solving the considered inverse problem to yield non-stationary processes of different effective durations achieving enhanced compatibility on the average with the GB 50011 spectrum. Therefore, the thus derived EPSs can significantly facilitate Monte Carlo-based or random vibration-based analyses in structural design scenarios where accounting for the effective duration is deemed essential (e.g. ASCE 2000, Hancock and Bommer 2007).

Commenting on the median peak factor spectra reported herein for uniformly modulated C-P and K-T processes three main conclusions can be drawn. First, once a specific parametric spectral form is adopted (i.e. either C-P or K-T), its frequency content does not significantly influence the peak factor spectra. Second, there is a large difference in peak factors corresponding to the C-P and K-T spectral forms in the region of flexible oscillators whose response is mostly influenced by the high-pass filter incorporated by the C-P spectrum. Third, the impact of the damping ratio on the median peak factors seems to be less significant than the impact of the duration of the input processes.

It is emphasized that the adopted formulation is not restricted to uniformly modulated processes which assume a constant in time frequency content. In fact, it can accommodate any analytically defined “fully non-stationary” (i.e. non-separable) EPS to be used to model

the evolutionary attributes observed in recorded strong ground motions. For instance, the non-separable EPS used in Spanos and Vargas Loli (1985) and more recently adopted by Conte and Peng (1997) could have been assumed (see also Cacciola 2010). This EPS is defined by a weighted sum of Kanai-Tajimi uniformly modulated processes and may potentially involve tenths of parameters to be determined. Alternative non-separable EPSs found in the literature may also be utilized in the same context (e.g. Preumont 1985b, Wen and Eliopoulos 1994, Wang et al. 2002, etc.). However, in this work the authors purposely refrained from considering such non-separable processes aiming at simplicity and practicality. This is because the purpose herein was not to capture/represent the strong ground motion in the best possible realistic fashion. Arguably, such a consideration is better addressed by means of time-frequency representation techniques (see e.g. Spanos et al. 2007a and Spanos et al. 2007b and references therein), or by means of adaptive (i.e. time-varying) filter models (see e.g. Fan and Ahmadi 1990, Rezaeian and Der Kiureghian 2010) applied to field recorded accelerograms. In this work, the uniformly modulated EPS is merely used as a mathematical instrument to achieve an acceptable level of matching between the sought processes and the target spectrum in the context set by codes of practice regulating the aseismic structural design.

### **Acknowledgments**

The partial support through the “Pump Priming Fund” granted by City University London is gratefully acknowledged by the first author.

### **Appendix A. Design spectra of the Chinese GB 50011 and the European EC8 codes**

The elastic relative displacement response/design spectrum for oscillators with damping ratio  $\zeta$  and natural period  $T$ , is defined in the current European aseismic code (EC8) by the expression (CEN, 2004)

$$S_d(T, \zeta_n) = \frac{1}{(2\pi)^2} a_g S \times \begin{cases} T^2 \left[ 1 + \frac{T}{T_B} (2.5\eta - 1) \right], & 0 \leq T \leq T_B \\ 2.5\eta T^2, & T_B \leq T \leq T_C \\ 2.5\eta T_C T, & T_C \leq T \leq T_D \\ 2.5\eta T_C T_D, & T_D \leq T \leq T_E \\ T_C T_D \left[ 2.5\eta + \frac{T - T_E}{T_F - T_E} (1 - 2.5\eta) \right], & T_E \leq T \leq T_F \\ T_C T_D, & T \geq T_F \end{cases}, \quad (\text{A.1})$$

where

$$\eta = \sqrt{\frac{10}{5 + \zeta_n}} \geq 0.55. \quad (\text{A.2})$$

In Eq. (A.1)  $a_g$  is the peak ground acceleration,  $S$  is an amplification factor dependent on the soil conditions, and  $T_B$ ,  $T_C$ ,  $T_D$ ,  $T_E$ , and  $T_F$  are the corner periods defining the various branches of the design spectrum also dependent on the soil conditions. The EC8 prescribes five different soil conditions to capture the influence of the surface soil layers resulting in different shapes as shown in Fig. 12

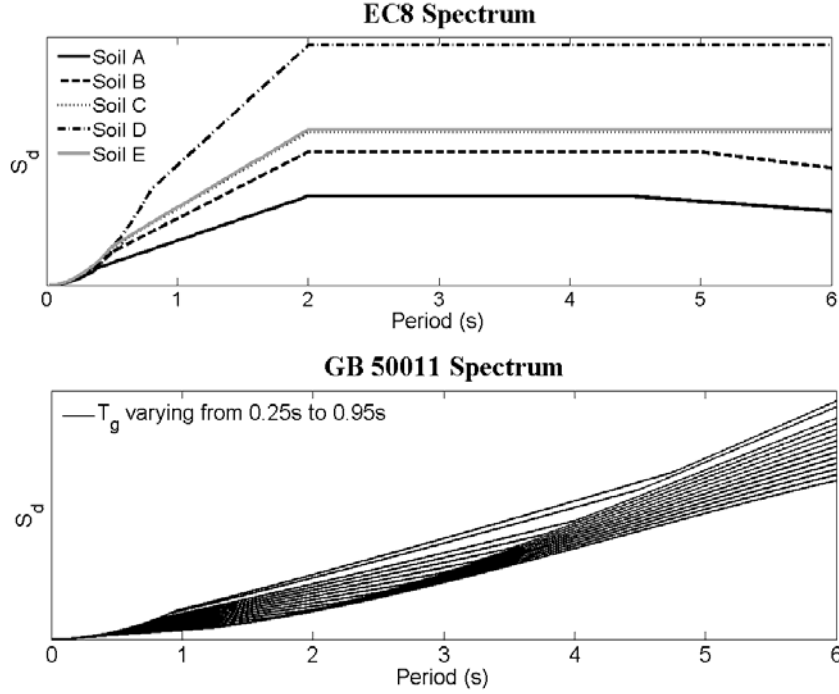


Fig. 12: EC8 and GB 50011 relative displacement elastic design spectra.

The elastic relative displacement design spectrum for oscillators with  $\zeta = 5\%$  and natural period  $T$ , is defined in the current aseismic code provisions effective in China (GB 50011, 2001) by the expression

$$S_d = \left(\frac{T}{2\pi}\right)^2 a_{\max} \times \begin{cases} (0.45 + 5.5T) & , 0 \leq T \leq 0.1 \\ 1 & , 0.1 \leq T \leq T_g \\ \left(\frac{T_g}{T}\right)^{0.9} & , T_g \leq T \leq 5T_g \\ \left(0.2^{0.9} - \frac{T - 5T_g}{50}\right) & , 5T_g \leq T \leq 6 \end{cases} \quad (\text{A.3})$$

In the above equation  $a_{\max}$  denotes the maximum spectral ordinate in terms of the pseudo-acceleration, and  $T_g$  is the “characteristic period” which differentiates the shape of the design spectrum to account for various soil conditions and intensity levels as defined by the GB 50011.  $T_g$  can take on 14 different values ranging from 0.25s to 0.95s which differentiate its shape as shown in Fig. 12.

## Appendix B. References

- ASCE (2000). “*Seismic analysis of safety-related nuclear structures and commentary*”, ASCE standard no. 004-98, American Society of Civil Engineers.
- ASCE (2006). “*Minimum design loads for buildings and other structures*”, ASCE standard no. 007-05, American Society of Civil Engineers.
- Bogdanoff, J. L., Goldberg, J. E. and Bernard, M. C. (1961), “Response of a simple structure to a random earthquake-type disturbance”, *Bull. Seism. Soc. Am.*, **51**, 293-310.
- Bommer, J.J. and Martínez-Pereira, A. (1999), “The effective duration of earthquake strong motion”, *J. Earthquake Eng.*, **3**, 127-172.
- Cacciola P. (2010), “A stochastic approach for generating spectrum compatible fully nonstationary earthquakes”, *Comp. Struct.* **88**, 889-901.
- CEN (2004). “*Eurocode 8: Design of Structures for Earthquake Resistance - Part 1: General Rules, Seismic Actions and Rules for Buildings*”, EN 1998-1: 2004, Comité Européen de Normalisation, Brussels.
- Chopra, A.K. (2007), “Elastic response spectrum: a historical note”, *Earthquake Eng. Struct. Dyn.*, **36**, 3-12.
- Clough, R.W. and Penzien, J. (1993), *Dynamics of Structures. Second Edition*. Mc-Graw Hill, New York.
- Conte, J.P. and Peng, B.F. (1997). “Fully nonstationary analytical earthquake ground-motion model”, *J. Eng. Mech., ASCE*, **123**: 15-24.
- Corotis, R.B., Vanmarcke, E.H. and Cornell, C.A. (1972), “First passage of nonstationary random processes”, *J. Eng. Mech. Div., ASCE*, **98**, 401-414.
- Crespi, P.G., Floris, C. and Paganini, P. (2002), “A probabilistic method for generating spectrum compatible earthquake time histories”, *Eur., Earthquake Eng.*, **16**(3): 3-17.

- Faccioli, E., Paolucci, R. and Rey, J. (2004), "Displacement spectra for long periods," *Earthquake Spectra*, **20**: 347-376.
- Falsone, G. and Neri, F. (2000), "Stochastic modeling of earthquake excitation following the EC8: power spectrum and filtering equations", *Eur., Earthquake Eng.*, **14**(1): 3-12.
- Fan, F.-G. and Ahmadi, G. (1990), "Nonstationary Kanai-Tajimi models for El Centro 1940 and Mexico City 1985 earthquakes", *Probab. Eng. Mech.*, **5**, 171-181.
- GB 50011 (2001). "Code for seismic design of buildings", National Standard of the People's Republic of China, China Building Industry Press, Beijing.
- Giaralis, A. and Spanos, P.D. (2009), "Wavelets based response spectrum compatible synthesis of accelerograms- Eurocode application (EC8)", *Soil Dyn. Earthquake Eng.*, **29**, 219-235.
- Giaralis, A. and Spanos P.D. (2010), "Effective linear damping and stiffness coefficients of nonlinear systems for design spectrum based analysis", *Soil Dyn. Earthquake Eng.*, **30**, 798-810.
- Gupta, I.D. and Trifunac, M.D. (1998), "Defining equivalent stationary PSDF to account for nonstationarity of earthquake ground motion", *Soil Dyn. Earthquake Eng.*, **17**, 89-99.
- Hancock, J. and Bommer, J.J. (2006), "A state-of-knowledge review of the influence of strong-motion duration on structural damage", *Earthquake Spectra*, **22**, 827-845.
- Hancock, J. and Bommer, J.J. (2007), "Using spectral matched records to explore the influence of strong-motion duration on inelastic structural response", *Soil Dyn. Earthquake Eng.*, **27**, 291-299.
- Iervolino, I., Maddaloni, G. and Cosenza, E. (2008), "Eurocode 8 compliant real records sets for seismic analysis of structures", *J. Earthquake Eng.*, **12**, 54-90.

- Jayaram, N., Lin T. and Baker, J.W. (2011), "A computationally efficient ground-motion selection algorithm for matching a target response spectrum mean and variance", *Earthquake Spectra*, **27**, 797-815.
- Kanai, K. (1957), "Semi-empirical formula for the seismic characteristics of the ground", *University of Tokyo, Bulletin of the Earthquake Research Institute*, **35**, 309-325.
- Katsanos, E.I., Sextos, A.G., Manolis, G.D. (2010), "Selection of earthquake ground motion records: A state-of-the-art review from a structural engineering perspective", *Soil Dyn. Earthquake Eng.*, **30**, 157-169.
- Kaul, M.K. (1978), "Stochastic characterization of earthquakes through their response spectrum", *Earthquake Eng. Struct. Dyn.*, **6**, 497-509.
- Kotz, S. and Nadarajah, S. (2000), *Extreme Value Distribution. Theory and Applications*. Imperial College Press, London.
- Martinelli, L., Barbella, G. and Feriani, A. (2011), "A numerical procedure for simulating the multi-support seismic response of submerged floating tunnels anchored by cables", *Eng. Struct.*, **33**, 2850-2860.
- Mason, A.B. and Iwan, W.D. (1983), "An approach to the first passage problem in random vibration", *J. Appl. Mech.*, ASME, **50**, 641-646.
- Michaelov, G., Lutes, L. D. and Sarkani, S. (2001), "Extreme value of response to nonstationary excitation", *J. Eng. Mech.*, ASCE, **127**, 352-363.
- Morikawa, H. and Zerva, A. (2008), "Approximate representation of the statistics for extreme responses of single degree-of-freedom system excited by non-stationary processes", *Probab. Eng. Mech.*, **23**, 279-288.
- Newmark, N.M. and Hall, J.W. (1982), *Earthquake spectra and design*, Earthquake Engineering Research Institute, Oakland.

- Nigam, N.C. and Jennings, P.C. (1969), "Calculation of response spectra from strong-motion earthquake records", *Bull. Seism. Soc. Am.*, **59**, 909-922.
- Nocedal, J. and Wright, S.J. (1999), *Numerical Optimization*, Springer-Verlag, New York.
- Preumont, A. (1985a), "The generation of non-separable artificial earthquake accelerograms for the design of nuclear power plants", *Nucl. Eng. Des.*, **88**, 59-67.
- Preumont, A. (1985b), "On the peak factor of stationary Gaussian processes", *J. Sound Vib.*, **132**: 457-471.
- Priestley, M.B. (1965). "Evolutionary Spectra and Non-Stationary Processes", *J. Royal Statistical Soc. Series B*, **27**, 204-237.
- Rezaeian, S. and Der Kiureghian, A. (2008), "A stochastic ground motion model with separable temporal and spectral nonstationarities", *Earthquake Eng. Struct. Dyn.*, **37**, 1565-1584.
- Roberts, J.B. and Spanos, P.D. (2003), *Random Vibration and Statistical Linearization*, Dover Publications, New York.
- Senthilnathan, A. and Lutes, L.D. (1991), "Nonstationary maximum response statistics for linear structures", *J. Eng. Mech., ASCE*, **117**, 294-311.
- Shrikhande, M. and Gupta, V.K. (1996), "On generating ensemble of design spectrum-compatible accelerograms", *Eur., Earthquake Eng.*, **10**(3), 49-56.
- Spanos, P.D. (1978), "Non-stationary random vibration of a linear structure", *International J. Solids Struct.*, **14**, 861-867.
- Spanos, P.D. and Lutes, L.D. (1980), "Probability of response to evolutionary process", *J. Eng. Mech. Div., ASCE*, **106**, 213-224.
- Spanos, P.D. and Vargias Loli, L.M. (1985), "A statistical approach to generation of design spectrum compatible earthquake time histories", *International J. Soil Dyn. Earthquake Eng.*, **4**, 2-8.

- Spanos, P.D. and Zeldin, B.A., (1998), "Monte Carlo treatment of random fields: A broad perspective", *Appl. Mech. Rev.*, **51**, 219-237.
- Spanos, P.D., Giaralis, A. and Politis, N.P. (2007a), "Time- frequency representation of earthquake accelerograms and inelastic structural response records using the adaptive chirplet decomposition and empirical mode decomposition", *Soil Dyn. Earthquake Eng.*, **27**: 675- 689.
- Spanos, P. D., Giaralis, A. and Jie, L. (2009), "Synthesis of accelerograms compatible with the Chinese GB 50011-2001 design spectrum via harmonic wavelets: artificial and historic records", *Earthquake Eng. Eng. Vibr.* **8**, 189-206.
- Spanos, P.D., Giaralis, A., Politis, N.P. and Roessett, J.M. (2007b), "Numerical treatment of seismic accelerograms and of inelastic seismic structural responses using harmonic wavelets", *Comp.-Aided Civil Infrastructure Eng.*, **22**, 254- 264.
- Taflanidis, A.A. and Jia, G. (2011), "A simulation-based framework for risk assessment and probabilistic sensitivity analysis of base-isolated structures", *Earthquake Eng. Struct. Dyn.*, **40**, 1629-1651.
- Trifunac, M.D. and Brady, A.G. (1975), "A study on the duration of strong earthquake ground motion", *Bull. Seism. Soc. Am.*, **65**, 581-626.
- Vanmarcke, E.H. (1976) Structural Response to Earthquakes. In C. Lomnitz & E. Rosenblueth, Eds., *Seismic Risk and Engineering Decisions*, Elsevier, Amsterdam, The Netherlands, 1976.
- Wang, J., Fan, L., Qian, S. and Zhou, J. (2002), "Simulations of non-stationary frequency content and its importance to seismic assessment of structures", *Earthquake Eng. Struct. Dyn.*, **31**, 993-1005.

Wen, Y.K. and Eliopoulos, D. (1994), "Method for nonstationary random vibration of inelastic structures", *Probab. Eng. Mech.*, **9**, 115-123.

Zembaty, Z. (1988), "A note on non-stationary stochastic response and strong motion duration", *Earthquake Eng. Struct. Dyn.*, **16**, 1189-1200.